

PAPER

DeepSun: machine-learning-as-a-service for solar flare prediction

To cite this article: Yasser Abdullaah *et al* 2021 *Res. Astron. Astrophys.* **21** 160

View the [article online](#) for updates and enhancements.

You may also like

- [Prediction of Flares within 10 Days before They Occur on the Sun](#)

Nasibe Alipour, Faranak Mohammadi and Hossein Safari

- [Solar Flare Predictive Features Derived from Polarity Inversion Line Masks in Active Regions Using an Unsupervised Machine Learning Algorithm](#)

Jingjing Wang, Yuhang Zhang, Shea A. Hess Webber *et al.*

- [Solar Flare Prediction with the Hybrid Deep Convolutional Neural Network](#)

Yanfang Zheng, Xuebao Li and Xinshuo Wang

DeepSun: machine-learning-as-a-service for solar flare prediction

Yasser Abdullaah^{1,2}, Jason T. L. Wang^{1,2}, Yang Nie^{1,2}, Chang Liu^{1,3,4} and Haimin Wang^{1,3,4}

¹ Institute for Space Weather Sciences, New Jersey Institute of Technology, University Heights, Newark, NJ 07102-1982, USA; wangj@njit.edu, haimin.wang@njit.edu

² Department of Computer Science, New Jersey Institute of Technology, University Heights, Newark, NJ 07102-1982, USA

³ Big Bear Solar Observatory, New Jersey Institute of Technology, 40386 North Shore Lane, Big Bear City, CA 92314-9672, USA

⁴ Center for Solar-Terrestrial Research, New Jersey Institute of Technology, University Heights, Newark, NJ 07102-1982, USA

Received 2020 September 18; accepted 2021 February 5

Abstract Solar flare prediction plays an important role in understanding and forecasting space weather. The main goal of the Helioseismic and Magnetic Imager (HMI), one of the instruments on NASA's Solar Dynamics Observatory, is to study the origin of solar variability and characterize the Sun's magnetic activity. HMI provides continuous full-disk observations of the solar vector magnetic field with high cadence data that lead to reliable predictive capability; yet, solar flare prediction effort utilizing these data is still limited. In this paper, we present a machine-learning-as-a-service (MLaaS) framework, called DeepSun, for predicting solar flares on the web based on HMI's data products. Specifically, we construct training data by utilizing the physical parameters provided by the Space-weather HMI Active Region Patch (SHARP) and categorize solar flares into four classes, namely B, C, M and X, according to the X-ray flare catalogs available at the National Centers for Environmental Information (NCEI). Thus, the solar flare prediction problem at hand is essentially a multi-class (i.e., four-class) classification problem. The DeepSun system employs several machine learning algorithms to tackle this multi-class prediction problem and provides an application programming interface (API) for remote programming users. To our knowledge, DeepSun is the first MLaaS tool capable of predicting solar flares through the internet.

Key words: Sun: flares — Sun: activity — methods: data analysis

1 INTRODUCTION

Solar flares and the often-associated coronal mass ejections (CMEs) highly impact the near-Earth space environment (Liu et al. 2017; Liu et al. 2020a). They have the potential to cause catastrophic damage to technology infrastructure (Daglis et al. 2004). According to the U.S. National Space Weather Strategy, released by the Space Weather Prediction Center, it is a challenging task to correctly predict solar flares and CMEs. Recent efforts led by the United States and its partners resulted in substantial progress toward monitoring, prediction and mitigation plans, but much more effort is still needed.

Research has shown that the magnetic free energy stored in the corona, quickly discharged by magnetic reconnection, powers solar flares and CMEs (Priest & Forbes 2002). The process of building the coronal

free energy is controlled by the structural evolution of the magnetic field on the photosphere where plasma dominates the process. Observing and measuring the structure and evolution of the photospheric magnetic field can provide valuable information and clues to the triggering mechanisms of flares and CMEs. There are many physical properties or parameters, as we will discuss later in the paper, that characterize the static photospheric magnetic field, such as integrated Lorentz force, magnetic helicity injection, unsigned magnetic flux, vertical electric currents, magnetic shear and gradient, and magnetic energy dissipation.

Researchers spent significant efforts attempting to understand the physical relationship between flare productivity and non-potentiality of active regions (ARs) as specified by the physical parameters. This led researchers to apply different methods to predict flares that are not

based on physical models, but rather based on statistical modeling and machine learning (Barnes et al. 2016). Machine learning gives computer programs the ability to learn from data and progressively improve performance. It utilizes input data, also called training data, and learns hidden insights in the training data to build a predictive model that will be used later to make predictions on unseen test data.

In our previous work (Liu et al. 2017), we reported the results of solar flare prediction using the random forest (RF) algorithm in Breiman et al. (1984). We constructed a database of solar flare events considering the physical parameters provided by the Space-weather HMI Active Region Patch (SHARP), and categorized solar flares into four different classes, namely B, C, M and X, based on the X-ray flare catalogs available at the National Centers for Environmental Information (NCEI)¹. We employed the RF algorithm and the physical parameters or features to perform multi-class classification of solar flares, predicting the occurrence of a certain class of flares in a given AR within 24 h.

In this paper, we extend our previous work in Liu et al. (2017) by considering two additional multi-class classification algorithms: multilayer perceptrons (MLPs) and extreme learning machines (ELMs). We implement these algorithms into a machine-learning-as-a-service (MLaaS) framework, called DeepSun, which allows scientists to perform multi-class flare prediction on the internet. Specifically, our work here makes two contributions.

1. We develop an ensemble (ENS) method for multi-class flare prediction that performs better than the existing machine learning algorithms including RF, MLP and ELM according to our experimental study.
2. We design and implement DeepSun, which is the first MLaaS system of its kind for solar flare prediction.

The rest of this paper is organized as follows. Section 2 describes the data and the SHARP predictive parameters used in this study. Section 3 describes the machine learning algorithms employed by DeepSun. Section 4 explains the methodology followed to evaluate the performance of these machine learning algorithms. Section 5 presents and compares the prediction results obtained from the machine learning algorithms. Section 6 details the design and implementation of the DeepSun framework. Section 7 surveys related work and compares DeepSun with existing computing systems providing similar services. Section 8 concludes the paper and points out some directions for future research.

¹ In the NCEI catalogs, the B class is the lowest flare class (Liu et al. 2017).

Table 1 Thirteen SHARP Parameters Used in Our Study

Parameter	Description
ABSNJZH	Absolute value of the net current helicity
AREA_ACR	Area of strong field pixels in the active region (AR)
EPSZ	Sum of z -component of normalized Lorentz force
MEANPOT	Mean photospheric magnetic free energy
R_VALUE	Sum of flux near polarity inversion line
SAVNCP	Sum of the modulus of the net current per polarity
SHRGT45	Fraction of area with shear $> 45^\circ$
TOTBSQ	Total magnitude of Lorentz force
TOTFZ	Sum of z -component of Lorentz force
TOTPOT	Total photospheric magnetic free energy density
TOTUSJH	Total unsigned current helicity
TOTUSJZ	Total unsigned vertical current
USFLUX	Total unsigned flux

2 DATA AND SHARP PARAMETERS

In 2012, SHARP data were released. The main goal of the SHARP data was to facilitate AR event forecasting (Bobra et al. 2014). These data are available in the Joint Science Operations Center (JSOC)² as `hmi.sharp` series which includes magnetic measures and parameters for many ARs. In 2014, another data series, `cgem.Lorentz`, was produced based on the SHARP data. This series includes the Lorentz force estimations. The main goal of this series was to help diagnose the dynamic process of ARs. Bobra et al. (2014) considered 25 physical parameters in the SHARP datasets that characterize the AR magnetic field properties. The authors relied on a univariate feature selection method to score the 25 parameters, and suggested that the top 13 out of the 25 parameters be regarded as predictors for flare activity. Table 1 summarizes these 13 parameters and their descriptions. More details about the 13 magnetic parameters can be found in Liu et al. (2017). Following Bobra et al. (2014) and Liu et al. (2017) we use the same 13 SHARP parameters in the work presented here.

We constructed a database based on the SHARP parameters extracted from the solar images that are available at JSOC and the X-ray flare catalogs provided by NCEI (Liu et al. 2017). We consider the period between May 2010 and December 2016. We select and record 845 flares in this period, among which 128 flares are of class B, 552 flares are of class C, 142 flares are of class M and 23 flares are of class X where identified locations of the C-, M- and X-class flares are within about $\pm 70^\circ$ of the central meridian (Liu et al. 2017). These 845 flares come from 472 ARs. The duration of a flare ranges from several minutes to hours. The duration of an AR ranges from days to months. If there are several flares from the same AR on the same day, the highest-class flare is recorded; if there are several highest-class flares on the same day, only the last such flare on that day is recorded. If two different ARs produce flares on the same day, the highest-class flare for each AR on

² <http://jsoc.stanford.edu/>

Table 2 Numbers of Flares and ARs per Solar Flare Class

Flare Class	Number of Flares	Number of ARs
B	128	88
C	552	281
M	142	88
X	23	15

that day is recorded separately. See section 2 of Liu et al. (2017) for more details on the criteria applied to select the 845 flares. Table 2 summarizes the flare information.

We created and stored 845 corresponding data samples (records) in our database, displayed in Figure 1 and accessible at <https://nature.njit.edu/spacesoft/Flare-Predict/>, where each data sample contains values of the 13 SHARP parameters or features listed in Table 1. Specifically, we created one data sample (record) for each flare. Thus, each record in our database has only one flare and corresponds to one date. The “Flare Date” column featured in Figure 1 indicates the first time on the flare date when all 13 SHARP parameter values are available, and the “Start Time” column indicates the start time of the flare on that date. Choosing SHARP parameter values measured at the beginning of the flare date is in accordance with our objective of predicting flares within 24 h. The two digits following a class label (B, C, M, X) are ignored in performing flare prediction. For simplicity, the two digits are specified without a dot (e.g., “B1.6” is specified as “B16”).

Because the 13 SHARP parameters have different scales and units, we normalize the parameter values as follows. Let \hat{x}_i^k (x_i^k , respectively) denote the normalized (original, respectively) value of the i^{th} parameter of the k^{th} data sample. Then

$$\hat{x}_i^k = \frac{x_i^k - \min_i}{\max_i - \min_i},$$

where \max_i (\min_i , respectively) is the maximum (minimum, respectively) value of the i^{th} parameter. The normalized values range from 0 to 1.

3 MACHINE LEARNING ALGORITHMS

DeepSun employs three machine learning algorithms for flare prediction: RFs (Breiman et al. 1984), MLPs (Rosenblatt 1958; Braspenning et al. 1995) and ELMs (Huang & Chen 2007, 2008). RF is a tree-based algorithm comprised of multiple binary classification and regression trees (CARTs) while both MLP and ELM are feed-forward artificial neural networks (ANNs; Braspenning et al. 1995). All the three algorithms are well suited for multi-class classification. In addition, we develop an ENS algorithm, which works by taking the majority vote of RF, MLP and ELM. When there is no majority vote for a test data sample, the ENS algorithm returns “no-verdict”. Since

there are three machine learning algorithms, this “no verdict” case occurs when the three algorithms assign the test data sample to three different classes.

We implemented the machine learning algorithms in Python leveraging the scikit-learn package (Pedregosa et al. 2011). Each algorithm has different optimization parameters to be tuned based on the training and test datasets. Our RF algorithm, which is the same as the one used in Liu et al. (2017), is composed of 1000 trees. We set the number of randomly chosen features to six when splitting a node to build a tree. The configurations and parameter settings of the MLP and ELM algorithms are described in detail below³. The parameter values were chosen to optimize the performance of each algorithm.

3.1 Multilayer Perceptrons

MLP is a variation of the single perceptron model originally introduced by Rosenblatt (1958). MLP consists of at least three layers: an input, an output, and one or several hidden layers. The number of hidden layers is a configuration parameter that can be adjusted by the user. MLP is a multi-class learning algorithm that can be applied for non-linearly separable problems. Each node, except the input nodes, is a neuron that incorporates a non-linear activation function. It utilizes back-propagation to calculate the weights used in the network’s activation function.

The MLP algorithm generally works as follows. We create weighted connections from each node in the input layer to each node in the first hidden layer h_1 . The process is repeated to create connections from subsequent hidden layer h_i to h_{i+1} until h_L where L is the total number of hidden layers. The connection from a node in a source layer, s_i , to a node in a target layer, t_i , is created with a weight w_i to generate a weighted sum that is passed to the next connection through the activation function. The weights of the connections are adjusted based on corrections that minimize the error in the entire output to produce the final result. We use the rectified linear unit (ReLU; Nair & Hinton 2010) as the activation function and optimize the log-loss function utilizing stochastic gradient descent where the log-loss is also known as the cross-entropy loss function. Most of the parameters in our MLP model are set with the default values provided by the scikit-learn library in Python (Pedregosa et al. 2011) except that the number of hidden layers is set to 200, the number of neurons in each hidden layer is set to 150, the learning rate is set to 0.001 and the batch size is set to 200.

³ The source code of the machine learning algorithms can be downloaded from <https://web.njit.edu/~wangj/MLaaS>.

Solar Flaring Active Region (AR) Database																		
There are 845 flare records in the period between May 2010 and December 2016. They are shown in the following table, which may be downloaded as a text file. Click the "Display Key" button to see the meaning of each column of the table. Click the "Search" button to search the database. See Liu et al. for the detailed methodology of sample selection and data retrieval used in this study.																		
Display Key Search Contact																		
Show <input type="button" value="10"/> entries per page																		
Flare Class	Flare Date	Start Time	AR #	TOTUSJH	TOTBSQ	TOTPOT	TOTUSJZ	ABSNJZH	SAVNCPP	USFLUX	AREA_ACR	TOTFZ	MEANPOT	R_VALUE	EPSZ	SHRG745		
B16	2016-12-27 00:10:30	1004	12621	487.186	3863200000	4.79623e22	10282700000000	50.024	1761570000000	3.33132e21	113.35	-438.15	6530.75	3.926	-0.2151	30.796		
B11	2016-12-11 13:58:31	1916	12617	26.477	1021300000	7.49059e20	368450000000	12.193	275278000000	1.86234e20	9.81402	-9.2336	2420.74	2.946	-0.0172	5.15		
B39	2016-11-30 00:10:32	0522	12614	330.547	4944100000	6.01896e22	6738150000000	83.429	1788770000000	3.83148e21	195.097	-389.43	7298.23	3.302	-0.1494	41.723		
M12	2016-11-29 00:10:32	2329	12615	380.206	5949000000	2.65588e22	6815700000000	8.078	2100250000000	4.31084e21	77.74	-1014	2541.43	3.5	-0.3233	9.864		
B19	2016-11-19 00:10:33	0710	12611	453.274	4039000000	2.45458e22	9979400000000	140.312	6265800000000	4.27975e21	159.167	-742.79	2668.6	3.011	-0.3488	10.699		
B42	2016-11-15 00:10:33	1653	12610	191.66	2753200000	1.59643e22	3697490000000	14.317	1201620000000	1.85299e21	196.69	-89.528	3684.01	3.219	-0.0617	23.996		
B11	2016-11-14 00:10:33	2337	12610	232.713	3162100000	2.12158e22	4480500000000	19.121	1189630000000	2.05412e21	156.076	-130.48	4417.92	3.101	-0.0783	27.904		
B15	2016-11-13 00:10:33	1729	12610	221.229	3246500000	1.69801e22	4603650000000	36.938	1227690000000	2.07567e21	100.11	-118.07	3630.26	2.698	-0.069	20.784		
B35	2016-10-16 00:10:37	1329	12602	226.128	4108000000	3.46127e22	4351460000000	21.034	1808050000000	2.74695e21	232.106	-340.65	6253.09	3.039	-0.1573	25.624		
C11	2016-10-12 00:10:38	1151	12599	2410.61	2694400000	3.76589e23	4622880000000	668.37	2283450000000	2.17183e22	997.74	-2589.2	8349.52	3.878	-0.1823	30.811		

Showing 1 to 10 of 845 entries

First Previous [1](#) [2](#) [3](#) [4](#) [5](#) Next Last**Fig. 1** Screenshot featuring our online flare database.

3.2 Extreme Learning Machines

ELM is a classification, regression and clustering algorithm that works for generalized single hidden layer feed-forward networks (Huang & Chen 2007, 2008). It has input, output and single or multiple hidden layers where hidden nodes' parameters do not need to be tuned. The parameters of the hidden nodes can randomly be assigned with non-linear transforms or inherited from their ancestors without being updated. In most cases, the output weights of ELM are learned in a single step which tends to be a linear model. ELM often has better scalability with a much faster learning speed.

The ELM algorithm generally works as follows. We determine the transfer function (activation function), the number of hidden layers, which is set to 1, and the number of neurons, which is set to 200, in the hidden layer. Then we assign weights and biases of neurons in the input layer where no tuning is needed. Finally we calculate the output weights. In our ELM model, we utilize the hyperbolic tangent (tanh) as the activation function and use the cross-entropy loss function with a regularized least squares solver.

4 PERFORMANCE EVALUATION METHODOLOGY

We conducted a series of experiments to evaluate the performance of the machine learning algorithms presented in Section 3 considering two types of datasets. The first type of dataset, referred to as original datasets, was obtained by duplicating the database described in Section 2 to create 100 identical copies of the database where each copy was an original dataset. Each original dataset contained 128 B-class, 552 C-class, 142 M-class and 23 X-class flares where each flare corresponded to a record in the dataset. There were 845 flares and hence 845 records in each original dataset. Totally there were 100 original

datasets. In addition, to mitigate the class imbalance problem that poses a major challenge in machine learning (see, e.g., Japkowicz & Stephen 2002), we created the second type of dataset, referred to as modified datasets, by randomly selecting 142 unique C-class flares from the total of 552 C-class flares. To avoid any bias, we repeated this random selection 100 times, so we ended up with 100 modified datasets, where each modified dataset contained 128 B-class, 142 C-class, 142 M-class and 23 X-class flares. Due to the few X-class flares, the modified datasets were still imbalanced datasets though they were not as unbalanced as the original datasets.

We used 10-fold cross validation in which for each dataset, we randomly shuffled to create 10-fold partitions using the KFold function provided by the scikit-learn library in Python (Pedregosa et al. 2011). Each machine learning algorithm was trained by nine of the 10 folds, and the 10th fold was used for testing. Notice that because the 10 folds in each original dataset were created randomly, the prediction results obtained from the 100 original datasets were different even though the 100 original datasets were identical. Notice also that each data sample (i.e., each record in our datasets) corresponded to one date and contained one flare. Each data sample either belonged to the training dataset or belonged to the testing dataset. There was no data sample belonging to both training and testing datasets. Thus, the testing data were not seen during training. To further reduce the errors associated with cross validation, we repeated the 10-fold cross validation procedure 100 times for each of the 100 original (modified, respectively) datasets, which resulted in 10 000 tests for the original (modified, respectively) datasets. The average values obtained from the 10 000 tests were calculated and reported.

In assessing the performance of the algorithms, we converted the multi-class classification problem at hand into four binary classification problems for the four classes

B, C, M and X respectively. For example, consider the binary classification problem for class B in a dataset. Here, we say a data sample is positive if it is in class B, or negative if it is not in class B, i.e., it is in class C, M or X. We define true positive (TP), false positive (FP), true negative (TN) and false negative (FN) as follows. TP is a data sample where an algorithm predicts the data sample to be positive and the data sample is indeed positive. FP is a data sample where the algorithm predicts the data sample to be positive while the data sample is actually negative. TN is a data sample where the algorithm predicts the data sample to be negative and the data sample is indeed negative. FN is a data sample where the algorithm predicts the data sample to be negative while the data sample is actually positive. We also utilize TP (FP, TN and FN respectively) to represent the number of true positives (false positives, true negatives and false negatives respectively).

Because we are tackling imbalanced classification problems, we adopt two performance metrics, balanced accuracy (BACC; Brodersen et al. 2010) and true skill statistics (TSS; Hanssen & Kuipers 1965). BACC is defined as follows

$$\text{BACC} = \frac{1}{2} \left(\frac{\text{TP}}{\text{TP} + \text{FN}} + \frac{\text{TN}}{\text{TN} + \text{FP}} \right),$$

and TSS is defined as follows

$$\text{TSS} = \frac{\text{TP}}{\text{TP} + \text{FN}} - \frac{\text{FP}}{\text{TN} + \text{FP}}.$$

BACC considers both sensitivity (also known as the true positive rate or recall) and specificity (also known as the true negative rate). It calculates the accuracy in the positive dataset and in the negative dataset separately, and is especially useful when the datasets are imbalanced, i.e., one dataset has many more elements than the other. In addition, because of its unbiasedness over the class-imbalance ratio (Woodcock 1976), we follow the suggestion of Bloomfield et al. (2012) to use the TSS score, which is the recall subtracted by the false alarm rate. We obtain BACC and TSS for each binary classification problem. There are four binary classification problems. We then calculate the average of the BACC and TSS values obtained from the four classification problems, and take the average as the result for the multi-class classification problem.

5 PREDICTION RESULTS

Table 3 (Table 4, respectively) compares the BACC and TSS values of the four machine learning algorithms presented in Section 3 for each binary classification problem and for the overall multi-class classification problem relying on the original (modified, respectively)

Table 3 Flare Prediction Results Using 13 SHARP Parameters and Four Machine Learning Algorithms on Original Datasets

	Class B	Class C	Class M	Class X	Average
BACC					
ENS	0.659	0.635	0.618	0.610	0.631
RF	0.635	0.630	0.590	0.580	0.608
MLP	0.616	0.620	0.584	0.575	0.599
ELM	0.629	0.619	0.586	0.573	0.601
TSS					
ENS	0.318	0.269	0.236	0.220	0.261
RF	0.271	0.259	0.179	0.160	0.217
MLP	0.231	0.241	0.169	0.150	0.198
ELM	0.259	0.238	0.172	0.146	0.204

Table 4 Flare Prediction Results Using 13 SHARP Parameters and Four Machine Learning Algorithms on Modified Datasets

	Class B	Class C	Class M	Class X	Average
BACC					
ENS	0.871	0.691	0.790	0.670	0.756
RF	0.834	0.663	0.749	0.645	0.723
MLP	0.818	0.659	0.757	0.599	0.708
ELM	0.791	0.641	0.721	0.608	0.690
TSS					
ENS	0.745	0.380	0.551	0.362	0.507
RF	0.708	0.378	0.537	0.330	0.488
MLP	0.661	0.285	0.526	0.010	0.371
ELM	0.618	0.296	0.446	0.227	0.397

datasets. In these tables, the highest performance metric values are highlighted in boldface. It can be seen from the tables that the proposed ENS algorithm outperforms the existing algorithms RF, MLP and ELM in both the original and modified datasets. Furthermore, the results from the modified datasets are better than those from the original datasets. This is due to the fact that the modified datasets have more balanced class distributions than the original datasets in the sense that the ratio of the number of X-class flares to the number of C-class flares is higher in the modified datasets than in the original datasets. It is worth noting that the performance of all the algorithms degrades in predicting X-class flares. This probably happens because the X class has much fewer flares than the other classes, and hence the algorithms cannot gain enough knowledge about the X-class flares. Overall, there were approximately less than 2% of data samples receiving “no verdict” in both the original and modified datasets.

6 THE DEEPSUN FRAMEWORK

6.1 System Design

The four machine learning algorithms (ENS, RF, MLP, ELM) presented in Section 3 have been implemented into our DeepSun system where the algorithms are utilized as

a back-end, also known as the server-side, engine for the MLaaS platform. Figure 2 presents the overall architecture of the DeepSun framework. The system supports two different types of users: web and programming. The web user invokes the service by accessing a graphical user interface (GUI) to perform flare predictions. The programming user can utilize any programming language that supports HTTP requests, such as Java, C++, Python, Node.js, JavaScript modules in React or other frameworks to perform flare predictions.

MLaaS is a representational state transfer (REST) application programming interface (API) that supports JavaScript Object Notation (JSON) formatted payloads in the request and response. JSON is a plain-text and lightweight data-interchange format. It is structured with attributes and values in an easy way for humans to read and write. JSON is language independent but it is easy to parse; therefore almost every programming language supports it. The request transmits the user's data from the front-end to the back-end and must include well defined JSON formatted test data to predict or training data to create a predictive model. The response transmits the result from the back-end to the front-end, which is a well formatted prediction result or the predictive model identifier. Here, the front-end means the client-side that can be a web-designed interface for the web user or a program for the programming user.

6.2 System Implementation

When a user visits DeepSun's home page, the user sees three options. Option 1 allows the user to select the pretrained models provided by DeepSun. Option 2 enables the user to upload his/her own training data to create his/her own machine learning models for solar flare prediction. Option 3 allows the user to perform solar flare prediction using RESTful services. Figure 3 features DeepSun's home page, which can be accessed at <https://nature.njit.edu/spacesoft/DeepSun/>.

6.2.1 Pretrained models in DeepSun

The pretrained models are ready-to-use models that were created utilizing the database described in Section 2. With the pretrained models, a user has three options to load test data samples containing the 13 SHARP parameters or features listed in Table 1: (1) Manually enter the data samples with values of the 13 SHARP parameters one by one in the provided text boxes. (2) Load sample data provided by the DeepSun engine. (3) Load the user's own data in a file, in which each line contains the values of the 13 SHARP parameters. The user may invoke the services to predict all the loaded, or entered, test data at once

or make predictions one by one. Figure 4 displays the webpage of pretrained models on which four predictions were made using the ENS algorithm.

6.2.2 Custom models in DeepSun

DeepSun allows the user to load his/her data to train and create his/her custom model to predict solar flares. The training data are saved in a file meeting DeepSun's format requirement. When the user creates a custom model, a model identifier (id) is assigned to the current session. If the created model is idle for 24 h, it will be deleted. Once the model is ready, the user goes to DeepSun's GUI with the assigned model id to perform flare predictions as done with the pretrained models. The model id is used to distinguish between the custom model and pretrained models. Figure 5 shows the webpage of custom models with example training data displayed.

6.2.3 RESTful API for DeepSun

Representational state transfer (REST) is an architectural style that defines rules for creating web services for an API. A web service application that implements and conforms to the REST architecture is referred to as a RESTful application. The RESTful application allows the user to interact with its system using http requests to access the data of the system in a well-defined format. Our RESTful API uses JSON, which is a lightweight format for storing and transmitting plain text data as described in Section 6.1.

The RESTful API helps the programming user perform solar flare predictions relying on the pretrained or custom models. The API supports the POST request to predict solar flare occurrence or create a custom model, and the GET request to get a random data sample from our training database. The interface supports JSON formatted strings for requests' body and their result. The interface also supports two different debug levels; they are (i) INFO which is the default debug mode and (ii) DEBUG to return additional data with the result.

The return result from the POST request is a JSON object including the predicted solar flare occurrence and its class. Each test data sample is associated with a JSON object that includes two attributes. One attribute is "fnumber" which is the numerical representation for the solar flare class where we define "1" ("2", "3", "4" respectively) to represent class B (C, M, X respectively). The other attribute is "fname" which is the solar flare class name.

In addition, the RESTful API utilizes the POST request to create a custom model. The body of the request must be JSON formatted strings for an array of JSON objects. Each object must contain the 13 SHARP

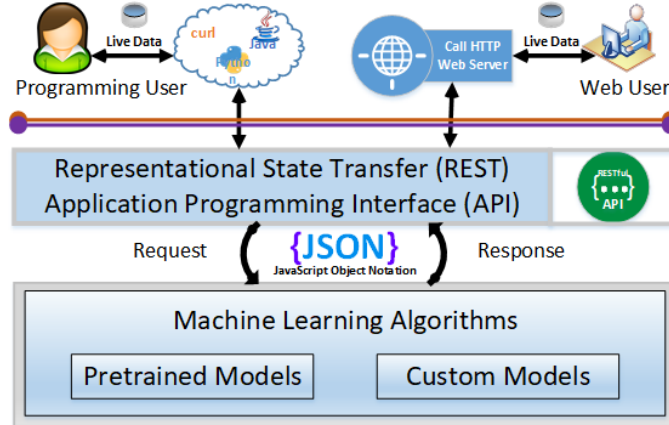


Fig. 2 Overview of DeepSun.

DeepSun

The DeepSun project encompasses a suite of automated machine learning tools available on the web for solar flare prediction. DeepSun offers three options. Option 1 allows the user to select the pretrained model provided by DeepSun. Option 2 allows the user to upload their own training data to create their own machine learning model for solar flare prediction. Option 3 allows the user to perform solar flare prediction using RESTful services.

Choose an option:

- Select the pretrained model provided by DeepSun
- Train using your data to create your model
- Learn how to use the RESTful services

[Next »](#)

Fig. 3 Screenshot depicting the home page of DeepSun.

Machine Learning as a Service (MLaaS) for Solar Flare Prediction

This MLaaS platform is designed to help users perform solar flare prediction as described in [Liu et al.](#) In addition to the user-friendly interface presented on this web page, an application programming interface (API) is also provided which can be accessed [here](#). The MLaaS platform offers users four prediction methods. These four methods are: (i) ensemble (ENS), (ii) random forests (RF), (iii) multilayer perceptrons (MLP), and (iv) extreme learning machines (ELM). ENS works by taking the majority vote of the results obtained from RF, MLP and ELM. The four prediction models are pretrained using the data described in [Liu et al.](#) which can be found in this [link](#). Click [here](#) to access another platform that allows users to train the machine learning models using their own training data.

Loading and predicting your test data:

There are three options to enter the data:

1. Manually enter the values of the 13 parameters one by one in the provided text boxes. Details of the 13 parameters can be found in [Liu et al.](#)
2. Load sample data provided by the MLaaS engine.
3. Load your own data in a file, in which each line must contain the values of the 13 parameters in the order specified in the table below. The file must be in the csv (comma-separated values) format and is limited to 200 lines or 50 KB, whichever is greater. Click [here](#) to see a sample test data file.

Select a prediction method:

ENS RF MLP ELM

Remove	TOTUSJH	TOTBSQ	TOTPOT	TOTUSJZ	ABSNJZH	SAVNCPP	USFLUX	AREA_ACR	TOTFZ	MEANPOT	R_VALUE	EPSZ	SHRG745	Class	Predict
Remove	999.258	168180000	2.17723e+24	7403000	38.46	147852000	1.22568e+	832.153	-595.26	6759.97	3.205	-0.0671	42.1	C	Submit
Remove	12172.3	252970000	5.22753e+	230024000	854.506	161343000	1.56972e+	6996.79	-9734.6	18097.8	5.332	-0.073	48.433	X	Submit
Remove	5351.32	116920000	1.22306e+	106392000	1099.74	283382000	7.87248e+	3169	-13116	7694.56	4.835	-0.2128	28.883	M	Submit
Remove	196.755	607720000	2.39097e+	275696000	10.256	750683000	4.44636e+	107.722	-1588.1	3943.85	3.004	-0.4957	3.067	B	Submit

Number of rows in test data table: 4

Fig. 4 Screenshot showing the webpage with pretrained models of DeepSun.

Machine Learning as a Service (MLaaS) for Solar Flare Prediction

Train using your own data and create your model

DeepSun allows you to load your data to train and create your model. Details concerning the training data can be found in [Liu et al.](#)

The data must be in the following format:

- Each row must contain the "Flare Class" label and the values of the 13 parameters as described in [Liu et al.](#). Note: Any additional parameters will be discarded.
- The "Flare Class" label must be one of the four letters: B, C, M, X, representing the four major flare classes as described in [Liu et al.](#).
- The file must be in the csv (comma-separated values) format and is limited to 650 KB.

Example training data are displayed below. You may copy and paste the data to a csv file or click the "Download training data" button below to download a sample csv file.

Flare Class, TOTUSJH, TOTB50, TOTPOT, TOTUSJZ, ABSNJZH, SAVNCPP, USFLUX, AREA_ACR, TOTFZ, MEANPOT, R_VALUE, EPSZ, SHRGTA45
B, 487.186, 3863200000, 4.80E22, 1.03E13, 50.024, 1.76E12, 3.33E21, 113.35, -438.15, 6530.75, 3.926, -0.2151, 30.796
B, 26.477, 1021300000, 7.49E20, 3.68E11, 12.193, 2.75E11, 1.86E20, 9.81402, -9.2336, 2420.74, 2.946, -0.0172, 5.15
B, 330.547, 4944100000, 6.02E22, 6.74E12, 83.429, 1.79E12, 3.83E21, 195.097, -389.43, 7298.23, 3.302, -0.1494, 41.723
M, 380.206, 5949000000, 2.66E22, 6.82E12, 8.078, 2.10E12, 4.31E21, 77.74, -1014, 3541.43, 3.5, -0.3233, 9.864
B, 453.274, 4039000000, 2.45E22, 9.98E12, 140.312, 6.27E12, 4.28E21, 159.167, -742.79, 2668.6, 3.011, -0.3488, 10.699
R, 191.66, 2753200000, 1.60F22, 3.70F12, 14.317, 1.20F12, 1.85F21, 196.69, -89.528, 3684.01, 3.219, -0.0617, 23.996

[Download training data](#)

Loaded file name: example_training_data.csv
File size: 5.28 KB
Label: Flare Class
List of parameters: TOTUSJH, TOTB50, TOTPOT, TOTUSJZ, ABSNJZH, SAVNCPP, USFLUX, AREA_ACR, TOTFZ, MEANPOT, R_VALUE, EPSZ, SHRGTA45
Model ID: nx0ea5sSvfaaEtR
Status: Completed and ready to use
Comments: Your created model must be used within 24 hours. If the created model is idle for 24 hours, it will be deleted.

[Upload training data](#) [Create your model](#) [Use your model](#) [Edit](#)

Fig. 5 Screenshot displaying the webpage with custom models of DeepSun.

parameters and its flare class label where the label must be one of B, C, M or X. The return result of this POST request is a JSON object that contains the custom model identifier (id) which can be exploited for flare prediction. The custom model includes all the four algorithms (ENS, RF, MLP, ELM). Since the API is a RESTful interface, any programming language that supports HTTP calls, such as Java, C++, Python, Node.js, JavaScript modules in React or other frameworks, can be used to invoke the API. Figure 6 depicts the RESTful API page on which the

definitions of the available methods and client examples are displayed.

We present a simple Python program for invoking the RESTful API to get a data sample (record) as shown in Listing 1 followed by another Python program to perform solar flare prediction as featured in Listing 2. More example programs can be found on our API main page accessible at <http://nature.njit.edu/spacesoft/MLaaS/api>.

Listing 1 Python Program to Get a Data Sample Using the DeepSun RESTful API

```

1 # import the requests library
2 import requests
3 # api-endpoint including the query parameter
4 URL = "https://nature.njit.edu/spacesoft/MLaaS/api/v1/data?query=getsampleddata"
5 # sending get request and saving the response as response object
6 r = requests.get(url = URL)
7 # saving data in json format
8 data = r.json()
9 print(data)

```

Listing 2 Python Program to Perform Solar Flare Prediction Using the DeepSun RESTful API

```

1 # import the requests and simplejson modules
2 import requests
3 import simplejson as json
4 # defining the api-endpoint
5 API_ENDPOINT = "https://nature.njit.edu/spacesoft/MLaaS/api/v1/predict"

```

```

6 # payload in JSON format data to be sent to api
7 # NOTE JSON is not python format; dumps and then loads, makes it JSON format
8 payload = '{"parameters":{"TOTUSJH":2699.42,"TOTBSQ":58985000000,"TOTPOT":1.07e+24,'
9 payload = payload + '"TOTUSJZ":53457900000000,"ABSNJZH":47.02,'
10 payload = payload + '"SAVNCPP":4510260000000,"USFLUX":3.58771e+22,'
11 payload = payload + '"AREA_ACR":1511.12,"TOTFZ":-3175.7,"MEANPOT":15255.1,'
12 payload = payload + '"R_VALUE":4.482,"EPSZ":-0.1021,"SHRGT45":49.982}}'
13 payload = json.dumps(payload)
14 payload = json.loads(payload)
15 print(payload)
16 # sending post request and saving response as response object
17 r = requests.post(url = API_ENDPOINT, data = payload)
18 print(r)
19 # saving response text
20 result=r.json()
21 print(result)

```

7 RELATED WORK

There are two groups of work that are closely related to ours. The first group is concerned with solar flare forecasting. Many studies in this group used parameters derived from the line-of-sight (LOS) component of the photospheric magnetic field and produced probability outputs for the occurrence of a certain magnitude flare in a time period (Liu et al. 2017). Some researchers (e.g., Gallagher et al. 2002) relied on sunspot classification and Poisson statistics to provide probabilities for an AR to produce flares with different magnitudes within 24 h. Song et al. (2009) used three LOS magnetic parameters together with the ordinal logistic regression (OLR) method to predict the probabilities of a one-day flare. Bloomfield et al. (2012) suggested that the prediction probabilities should be converted into a binary (i.e., yes-or-no) forecast before they can be translated as flare-imminent or flare-quiet. Following this suggestion, Yuan et al. (2010) employed support vector machines (SVMs) to obtain a clear true or false flare prediction for different flare classes.

On the other hand, the full vector data provide more information about the photospheric magnetic field structure compared to the LOS field. This type of information may provide better flare prediction performance, but due to the limitation imposed by ground-based vector magnetic field observations, the work on flare forecasting is limited. For example, Leka & Barnes (2003) utilized a small sample of vector magnetograms from the Mees Solar Observatory and applied a discriminant analysis to differentiate between flare-producing and flare-quiet ARs within a few hours. The authors later extended their work and used a larger number of samples with a 24-hr prediction window to generate probabilistic forecasts (Barnes et al. 2007).

Since May 2010, the Helioseismic and Magnetic Imager (HMI) onboard the Solar Dynamics Observatory (SDO) has been producing high quality photospheric vector magnetograms with high-cadence and full-disk

coverage data (Bobra & Couvidat 2015). Relying on these data, Bobra & Couvidat (2015) calculated a number of magnetic parameters for each AR. They selected 13 from all the available parameters and achieved good prediction performance utilizing an SVM method for flares greater than M1.0 class. Nishizuka et al. (2017) applied a number of machine learning algorithms to HMI data and produced prediction models for $\geq M$ and X-class flares with reasonably high performance. More recently, we employed a long short-term memory network for flare prediction (Liu et al. 2019).

The second group of related work is concerned with services computing. Benmerar et al. (2018) developed a brain diffusion magnetic resonance imaging (MRI) application to overcome the software-as-a-service (SaaS) limitations caused by intensive computation. The application provides APIs that tackle browser paradigms to reduce the parallel computation rendered in the client side of the browser.

Wu et al. (2018) developed an automated testing technique to detect cross-browser compatibility issues so that they can be fixed. These cross-browser issues cause problems for an organization to create JavaScript web applications. The authors employed an existing record-and-play technique, Mugshot (Mickens et al. 2010), to design an incremental cross-browser incompatibility algorithm. The system starts off by injecting the record library into the browsers, collects traces and events to be replayed, and runs the detection algorithm to find different types of incompatibilities among the browsers.

Song et al. (2012) presented a machine learning algorithm for IT support services to automate the problem of determination and classification, and also find the root cause of such a problem. The algorithm is an online perceptron that learns about the user's problems from the data that were generated from logs and monitors information across different systems. The algorithm then categorizes the problems by finding the actual root cause from what it learned from the data. The algorithm

Machine Learning as a Service (MLaaS) API for Solar Flare Prediction

This MLaaS API (application programming interface) is designed to help users perform solar flare prediction as described in [Liu et al.](#) The MLaaS API offers users four prediction methods. These four methods are: (i) ensemble (ENS), (ii) random forests (RF), (iii) multilayer perceptrons (MLP), and (iv) extreme learning machines (ELM). ENS works by taking the majority vote of the results obtained from RF, MLP and ELM. The four prediction models are pretrained using the data described in [Liu et al.](#) which can be found in this [link](#). This RESTful interface supports flare prediction using the pretrained models provided by DeepSun or your own custom model that is trained and created with your data. The API supports POST request to predict solar flare occurrence and GET request to get a random data sample from our training dataset.

Specifications:

Base URL	https://nature.njit.edu/spacesoft/MLaaS/api
Primary category	Solar flares
API provider	DeepSun
Schemes	HTTPS
Authentication	No authentication is required.
Client	Any programming language that supports HTTP calls, such as Java, C++, Python, Node.js, JavaScript modules in React or other frameworks, etc. can be used to invoke the API.

Request Methods Definitions:

Pretrained Model use our pretrained model.

POST	/spacesoft/MLaaS/api/v1/predict	Predict solar flare occurrence.	
GET	/spacesoft/MLaaS/api/v1/data	Get a test data record sample.	

Custom Model create your own model.

POST	/spacesoft/MLaaS/api/v1/train	Train your data and create your own model.	
-------------	--	--	--

Client Examples:

In this section, we provide GET and POST client examples using Python, Java, and curl command.

Python client	
Java client	
curl client	

Fig. 6 Screenshot showing the RESTful API page of DeepSun.

employs an incremental learning technique and is able to automatically adjust the classifier parameters.

[Li et al. \(2018\)](#) described a new software documentation recommendation methodology that adopts a learn-to-rank (LTR) technique. LTR is an application of supervised and semi-supervised machine learning techniques. Their strategy combines the social context from a question-and-answer online system and the content of official software documentation to build the LTR model to provide accurate and relevant software documentation recommendations. Their experimental results demonstrated that this approach outperforms traditional code search engines including the Google search engine.

Our DeepSun system differs from the above works in two ways. First, DeepSun provides services dedicated to solar flare prediction, which has not been addressed by the existing services computing systems. Second, in the solar flare forecasting area, DeepSun is the first MLaaS system, to our knowledge, that allows scientists to perform multi-class flare predictions through the internet.

8 CONCLUSIONS AND FUTURE WORK

We present an MLaaS framework (DeepSun) for solar flare prediction. This framework provides two interfaces:

a web server where the user enters the information through a GUI and a programmable interface that can be used by any RESTful client. DeepSun employs four machine learning algorithms, namely the RF, MLP, ELM and ENS algorithms. Our experimental results demonstrated good performance of the ENS algorithm and its superiority over the other three machine learning algorithms.

In our work, we rely on the database constructed in [Liu et al. \(2017\)](#), which contains 845 data samples belonging to four flare classes: B, C, M and X across 472 ARs. These data samples are unevenly distributed. Specifically, there are 128 B-class, 552 C-class, 142 M-class and 23 X-class flares where each flare corresponds to a data sample. To mitigate the class imbalance problem, we create modified datasets by randomly selecting 142 unique C-class flares from the total of 552 C-class flares. Balancing the data samples changes the flare occurrence frequency but provides better performance results as shown in Section 5. Our goal here is to gain a better understanding of the relative performance of the four machine learning algorithms in dealing with different imbalanced datasets. The models studied here are mainly used for scientific purposes, not for operations.

Because there are four flare classes, we perform four-class classification to predict which class of flares would

occur within 24 h. In practice, it is likely that there is no flare within 24 hr. To handle this situation, we adopt a two-step method. In the first step, a test record is fed to a binary classification model, which is similar to the binary classification tools described in Liu et al. (2019). This binary classification model predicts whether or not there is a flare within 24 h. If the prediction outcome is “no”, then the test record represents a non-flare event, meaning there is no flare within 24 h. If the prediction outcome is “yes”, then we enter the second step where we feed the test record to the DeepSun tool presented here to further identify which flare class the test record belongs to. If the test record is classified into class B (C, M or X), then we predict there is a B (C, M or X) class flare within 24 h.

In the current work, we focus on data samples composed of SHARP parameters. The HMI aboard the SDO also produces continuous full-disk observations (solar images). In future work, we plan to incorporate these HMI images into our DeepSun framework and extend our previously developed deep learning techniques (Hu et al. 2018, 2020; Liu et al. 2020b) to directly process the images. We also plan to combine our recently developed deep learning algorithms using the SHARP parameters (Liu et al. 2019) with the image-based techniques and machine learning algorithms described in this paper for more accurate solar flare prediction.

Acknowledgements We thank the referee for very helpful and thoughtful comments. We also thank the SDO/HMI team for producing vector magnetic field data products. The X-ray flare catalogs were prepared by and made available through NOAA NCEI. This work was supported by U.S. NSF grants AGS-1927578 and AGS-1954737. C.L. and H.W. acknowledge the support of NASA under grants NNX16AF72G, 80NSSC18K0673 and 80NSSC18K1705.

References

Barnes, G., Leka, K. D., Schumer, E. A., & Della-Rose, D. J. 2007, Space Weather, 5, S09002

Barnes, G., Leka, K. D., Schrijver, C. J., et al. 2016, The Astrophysical Journal, 829, 89

Benmerar, T. Z., Megherbi, T., Kachouane, M., Deriche, R., & Boumghar, F. O. 2018, IEEE Transactions on Services Computing

Bloomfield, D. S., Higgins, P. A., McAteer, R. T. J., & Gallagher, P. T. 2012, ApJ, 747, L41

Bobra, M. G., & Couvidat, S. 2015, ApJ, 798, 135

Bobra, M. G., Sun, X., Hoeksema, J. T., et al. 2014, Solar Physics, 289, 3549

Braspenning, P. J., Thuijsman, F., & Weijters, A. J. M. M., eds. 1995, Lecture Notes in Computer Science, 931, Artificial Neural Networks: An Introduction to ANN Theory and Practice (Springer)

Breiman, L., Friedman, J. H., & Olshen, R. A. 1984, Classification and Regression Trees (CA: Wadsworth International Group)

Brodersen, K. H., Ong, C. S., Stephan, K. E., & Buhmann, J. M. 2010, in Proceedings of the 20th International Conference on Pattern Recognition, 3121

Daglis, I., Baker, D., Kappenman, J., Panasyuk, M., & Daly, E. 2004, Space Weather, 2, S02004

Gallagher, P. T., Moon, Y.-J., & Wang, H. 2002, Solar Physics, 209, 171

Hanssen, A. W., & Kuipers, W. J. A. 1965, Meded. Verh, 81, 2

Hu, Z., Turki, T., Phan, N., & Wang, J. T. L. 2018, IEEE Access, 6, 43450

Hu, Z., Turki, T., & Wang, J. T. L. 2020, IEEE Access, 8, 63336

Huang, G.-B., & Chen, L. 2008, Neurocomputing, 71, 3460

Huang, G., & Chen, L. 2007, Neurocomputing, 70, 3056

Japkowicz, N., & Stephen, S. 2002, Intelligent Data Analysis, 429

Leka, K. D., & Barnes, G. 2003, The Astrophysical Journal, 595, 1296

Li, J., Xing, Z., & Kabir, A. 2018, IEEE Transactions on Services Computing

Liu, C., Deng, N., Wang, J. T. L., & Wang, H. 2017, ApJ, 843, 104

Liu, H., Liu, C., Wang, J. T. L., & Wang, H. 2019, ApJ, 877, 121

Liu, H., Liu, C., Wang, J. T. L., & Wang, H. 2020a, ApJ, 890, 12

Liu, H., Xu, Y., Wang, J., et al. 2020b, ApJ, 894, 70

Mickens, J., Elson, J., & Howell, J. 2010, in Proceedings of the 7th USENIX Symposium on Networked Systems Design and Implementation (NSDI 10) (San Jose, CA: USENIX Association)

Nair, V., & Hinton, G. E. 2010, in Proceedings of the 27th International Conference on Machine Learning (ICML-10), June 21-24, 2010, Haifa, Israel, eds. J. Fürnkranz, & T. Joachims (Omnipress), 807

Nishizuka, N., Sugiura, K., Kubo, Y., et al. 2017, ApJ, 835, 156

Pedregosa, F., Varoquaux, G., Gramfort, A., et al. 2011, Journal of Machine Learning Research, 12, 2825

Priest, E., & Forbes, T. 2002, The Astronomy and Astrophysics Review, 10, 313

Rosenblatt, F. 1958, The Perceptron: A Theory of Statistical Separability in Cognitive Systems (Cornell Aeronautical Laboratory, Inc., Rept. No. VG-1196-G-1)

Song, H., Tan, C., Jing, J., et al. 2009, Solar Physics, 254, 101

Song, Y., Sailer, A., & Shaikh, H. 2012, IEEE Transactions on Services Computing, 5, 345

Woodcock, F. 1976, Monthly Weather Review, 104, 1209

Wu, G., He, M., Chen, W., Wei, J., & Zhong, H. 2018, IEEE Transactions on Services Computing

Yuan, Y., Shih, F., Jing, J., & Wang, H. 2010, RAA (Research in Astronomy and Astrophysics), 10, 785